2-19-2013

Adsorption of Hydrogen on Neutral and Charged Fullerene: Experiment and Theory

Alexander Kaiser
University of Innsbruck

Christian Leidlmair
University of Innsbruck

Peter Bartl
University of Innsbruck

Samuel Zottl
University of Innsbruck

Stephan Denifl
University of Innsbruck

See next page for additional authors

Recommended Citation

A. Kaiser, C. Leidlmair, P. Bartl, S. Zöttl, S. Denifl, A. Mauracher, M. Probst, P. Scheier, and O. Echt, Adsorption of Hydrogen on Neutral and Charged Fullerene: Experiment and Theory, J. Chem. Phys. 138 (2013) 074311, DOI: 10.1063/1.4790403, Feb 2013

Adsorption of hydrogen on neutral and charged fullerene: Experiment and theory

Cite as: J. Chem. Phys. **138**, 074311 (2013); https://doi.org/10.1063/1.4790403
Submitted: 29 November 2012 . Accepted: 22 January 2013 . Published Online: 19 February 2013

A. Kaiser, C. Leidlmair, P. Bartl, S. Zöttl, S. Denifl, A. Mauracher, M. Probst, P. Scheier, and O. Echt

Adsorption of hydrogen on neutral and charged fullerene: Experiment and theory

A. Kaiser,[1] C. Leidlmair,[1] P. Bartl,[1] S. Zöttl,[1] S. Denifl,[1] A. Mauracher,[1] M. Probst,[1] P. Scheier,[1,a)] and O. Echt[1,2,a)]

[1]*Institut für Ionenphysik und Angewandte Physik, University of Innsbruck, Technikerstrasse 25, A-6020 Innsbruck, Austria*

[2]*Department of Physics, University of New Hampshire, Durham, New Hampshire 03824, USA*

(Received 29 November 2012; accepted 22 January 2013; published online 19 February 2013)

Helium droplets are doped with fullerenes (either C_{60} or C_{70}) and hydrogen (H_2 or D_2) and investigated by high-resolution mass spectrometry. In addition to pure helium and hydrogen cluster ions, hydrogen-fullerene complexes are observed upon electron ionization. The composition of the main ion series is $(H_2)_nHC_m^+$ where $m = 60$ or 70. Another series of even-numbered ions, $(H_2)_nC_m^+$, is slightly weaker in stark contrast to pure hydrogen cluster ions for which the even-numbered series $(H_2)_n^+$ is barely detectable. The ion series $(H_2)_nHC_m^+$ and $(H_2)_nC_m^+$ exhibit abrupt drops in ion abundance at $n = 32$ for C_{60} and 37 for C_{70}, indicating formation of an energetically favorable commensurate phase, with each face of the fullerene ion being covered by one adsorbate molecule. However, the first solvation layer is not complete until a total of 49 H_2 are adsorbed on C_{60}^+; the corresponding value for C_{70}^+ is 51. Surprisingly, these values do not exhibit a hydrogen-deuterium isotope effect even though the isotope effect for H_2/D_2 adsorbates on graphite exceeds 6%. We also observe doubly charged fullerene-deuterium clusters; they, too, exhibit abrupt drops in ion abundance at $n = 32$ and 37 for C_{60} and C_{70}, respectively. The findings imply that the charge is localized on the fullerene, stabilizing the system against charge separation. Density functional calculations for C_{60}-hydrogen complexes with up to five hydrogen atoms provide insight into the experimental findings and the structure of the ions. The binding energy of physisorbed H_2 is 57 meV for $H_2C_{60}^+$ and $(H_2)_2C_{60}^+$, and slightly above 70 meV for $H_2HC_{60}^+$ and $(H_2)_2HC_{60}^+$. The lone hydrogen in the odd-numbered complexes is covalently bound atop a carbon atom but a large barrier of 1.69 eV impedes chemisorption of the H_2 molecules. Calculations for neutral and doubly charged complexes are presented as well. © *2013 American Institute of Physics*. [http://dx.doi.org/10.1063/1.4790403]

I. INTRODUCTION

The adsorption of permanent gases on graphite, graphene, nanotubes, layers of fullerenes, and other graphitic materials has attracted considerable interest. One factor that drives research in this field is the need to develop the foundations for a hydrogen economy.[1] The use of hydrogen as an energy carrier requires the development of methods to store hydrogen in low-weight containers at high density and low cost, especially if hydrogen is to be used for transportation.[2] Storage of hydrogen gas in liquid form at high pressures and cryogenic temperatures is not likely to meet the performance targets of the US Department of Energy, and invokes safety hazards.[3] Better alternatives may be offered by absorption of H_2 to form metal hydrides, by chemical reactions, or by adsorption in porous, light-weight materials with large specific surface areas.[3,4] Although the physisorption energy of H_2 in pristine carbon-based materials, such as graphene, nanotubes, or fullerenes is only around 50 meV, the introduction of defects, dopants, or charges may raise adsorption energies sufficiently to allow for efficient storage at moderate pressures near ambient temperatures.[5,6]

Furthermore, hydrogen physisorbed on graphite or graphite-like materials exhibits strong corrugation effects, i.e., the interaction between the adsorbate and the substrate is much stronger than the interaction between adsorbate molecules.[7] This favors the formation of ordered layers which are commensurate with the arrangement of the carbon atoms in the honeycomb lattice of graphite, within certain ranges of coverage and temperature. H_2 molecules on graphite form a relatively simple phase diagram (coverage plotted versus temperature), with the appearance of just one commensurate phase, namely, the $\sqrt{3}\times\sqrt{3}$ phase in which 1/3 of all sites (all second-nearest neighbor sites) over the centers of the hexagonal carbon rings are occupied.[8] The same phase occurs for D_2 on graphite, but the lower zero-point energy of D_2 results in a much richer phase diagram; several other phases can be distinguished with increasing coverage.[9] The large isotope effect also results in a significantly higher density when the first monolayer is completed, namely, at 0.0987 $D_2/Å^2$ (or 1.55 times the coverage of the $\sqrt{3}\times\sqrt{3}$ phase) *versus* 0.0927 $H_2/Å^2$.

An intriguing question is the existence of related effects for H_2 and D_2 adsorbed on free fullerenes. Is the corrugation strong enough to favor an arrangement where each carbon ring is occupied by exactly one molecule? Are the molecules

a)paul.scheier@uibk.ac.at and olof.echt@unh.edu.

small enough to form a commensurate layer when each facet of the fullerene is occupied by one molecule, i.e., when 32 molecules are adsorbed on C_{60}? This phase would have a hydrogen-to-carbon ratio three times that of the $\sqrt{3}\times\sqrt{3}$ phase on graphite; it may be viewed as the 1×1 phase which does not form on graphite because H_2, He, and other physisorbed atoms or molecules are too large. The first complete monolayer on C_{60} may even accommodate additional molecules which would displace the other molecules from their registered sites.[10,11] The number of molecules in this incommensurate solvation layer could be subject to an isotope effect similar to the ≈6% isotope effect for the H_2/D_2 monolayer on graphite; the D_2 solvation shell could thus accommodate two or three molecules more than the H_2 solvation shell.

In a recent letter, we presented first evidence for the formation of positively charged H_2-fullerene physisorption complexes and discussed their possible presence in the interstellar medium.[12–15] Hydrogen is the most abundant element in the universe; 92% of all atoms in the universe are hydrogen.[16] Kroto *et al.*[17] had already conjectured that fullerenes or their derivatives may be major constituents of circumstellar shells with high carbon content or interstellar dust, catalyze reactions of new molecules in space, and be the carrier of the diffuse interstellar bands (DIBs), but early mass spectrometric evidence for extraterrestrial fullerenes in the carbonaceous impact residue in a crater on a spacecraft[18] or spectroscopic identification of fullerene cations in interstellar absorption bands[19] remained ambivalent.[20,21] Hydrogen inhibits the formation of fullerenes in an arc discharge[22] but very high (≥3500 K) temperatures may lead to fullerenes even if hydrogen is present.[23] Interstellar fullerenes may also originate from the envelopes surrounding mass-losing, hydrogen-deficient carbon-rich stars such as R Coronae Borealis (RCB).[20]

Recently, conclusive spectroscopic evidence for the existence of cold neutral fullerenes has been identified in IR spectra recorded by the Spitzer Space telescope in planetary nebulae.[24] Remarkably, they are estimated to represent a few percent of the total available cosmic carbon in those regions. Since then, neutral fullerenes have also been detected in a protoplanetary nebula,[25] the interstellar medium,[26] around RCB stars,[27] young stellar objects, and a pre-main-sequence star.[28] With an estimated energy of 50 meV for physisorption of H_2 on fullerenes, H_2 concentrations up to $\approx 10^4$ cm^{-3} and temperatures as low as 10 K in interstellar clouds,[29] we concluded that neutral or charged fullerene-hydrogen complexes are likely to occur in the interstellar medium, at least in the colder regions of dense molecular clouds.[12] The effect of one or more physisorbed H_2 molecules on the absorption spectra would have important ramifications for their possible contribution to the diffuse interstellar bands. The number of these bands, discovered 90 years ago by Heger as broad absorption features superimposed on the interstellar extinction curve[30] now exceeds 400[31] but they have not yet found a satisfactory, coherent explanation.[32]

In our recent letter,[12] we discussed the appearance of two ion series, namely, "even-numbered" $(H_2)_nC_m^+$ and "odd-numbered" $(H_2)_nHC_m^+$ where $m = 60$ or 70. Both ion series exhibit an abrupt drop in the abundance at $n = 32$ and 37 for C_{60} and C_{70}, respectively, which we attributed to an enhanced stability of the commensurate phase of the adsorbate, when each carbon ring is occupied by one hydrogen molecule. In our current work, we present additional experimental findings, together with *ab initio* calculations. In particular, we offer evidence for completion of a first hydrogen monolayer well beyond the completion of the commensurate phase, with no detectable isotope effect. Moreover, we show that doubly charged ions $(H_2)_nHC_m^{2+}$ also form a commensurate phase. Our *ab initio* calculations reveal the structure and energetics of small, neutral, and singly or doubly charged C_{60}-hydrogen complexes; they provide a rational for the relatively large abundance of even-numbered $(H_2)_nC_{60}^+$.

II. EXPERIMENT

Neutral helium nanodroplets are produced by expanding helium (purity 99.9999%) from a stagnation pressure of 2 MPa through a 5 μm nozzle, cooled to about 8 K by a closed-cycle refrigerator (Sumitomo Heavy Industries LTD, model RDK-415D), into vacuum. The estimated average number of helium atoms per droplet formed in the expansion is of the order of 5×10^5; the droplets are superfluid with a temperature of ≈0.37 K.[33] The resulting supersonic beam is skimmed by a 0.8 mm conical skimmer, located 8 mm downstream from the nozzle. The skimmed beam traverses a 20-cm long differentially pumped pickup region into which hydrogen (Messer Austria GmbH, specified purity 99.999%) or deuterium (99.7% by weight) are introduced; the measured partial pressure is typically a few times 10^{-3} Pa (uncorrected gauge signal). A small amount of C_{60} (MER Corp., 99.9%) or C_{70} (SES Research, 99%) is vaporized into the pickup region from a crucible. The temperature of the fullerene source is adjusted to optimize the pickup of just one fullerene per helium droplet.

After the pickup region, the doped helium droplets pass a region in which they are ionized by electron impact at 70 eV. Cations are accelerated to 40 eV into the extraction region of a commercial time-of-flight mass spectrometer equipped with a reflectron (Tofwerk AG, model HTOF); its mass resolution is about $\Delta m/m = 1/5000$. The base pressure in the mass spectrometer is 10^{-5} Pa. The ions are extracted at 90° into the field-free region of the spectrometer by a pulsed extraction voltage. At the end of the field-free region, they enter a two-stage reflectron which reflects them towards a microchannel plate detector operated in single ion counting mode. Additional experimental details have been described in Refs. 12 and 34.

III. DATA ANALYSIS: ION YIELD VERSUS ION ABUNDANCE

Mass spectra are analyzed by determining the ion yield, i.e., the amplitude of each mass peak, properly corrected for background. For strong mass peaks that are well separated from adjacent peaks we simply read the ion yield at its maximum, and in the valleys between adjacent peaks. For more problematic peaks that have either poor statistics or adjacent

peaks that are not well resolved, we apply nonlinear curve fitting to determine the background-corrected peak amplitude.

In the present study, mass peaks usually contain significant contributions from two or more different ions because of the ^{13}C isotope (mass 13.00335 u, natural abundance 1.07%). In order to extract the *abundance* of, say, $H_xC_{70}^+$, one needs to correct the measured *ion yield* for contributions from ions with smaller x that contain one or more ^{13}C (the presence of deuterium, natural abundance 0.0115%, may be neglected). The isotopically pure $H_x{}^{12}C_{70}^+$ will form a mass peak at $1.008725x + 70 \times 12$ u, while $H_{x-1}{}^{13}C^{12}C_{69}^+$ (which for convenience we will write as $H_{x-1}C_{70}^+$ $(1-{}^{13}C)$) will appear at $1.008725(x-1) + 69 \times 12 + 13.00335$ u, just 0.0054 u lower. This mass difference is much smaller than the width of the mass peak which measures ≈0.2 u (full-width-at-half-maximum, FWHM) at a mass of 1000 u. The contributions from these two ions will simply add, together with contributions from $H_{x-2}C_{70}^+$ $(2-{}^{13}C)$, etc.

If the abundance A_x of all ions $H_xC_{70}^+$ $(0-{}^{13}C)$ were known, the ion yield Y_x at nominal mass $x + 840$ u would follow from the relation

$$Y_x = \sum_{i=0}^{x} P_i A_{x-i}, \tag{1}$$

where P_i is the known probability of the C_{70} $(i-{}^{13}C)$ isotopologue. If carbon were monoisotopic one would simply have $P_0 = 1, P_1 = P_2 = \ldots = 0$, and $Y_x = A_x$.

Figure 1 illustrates the relation between ion yield and ion abundance. Panel (a) displays the abundance of $H_xC_{70}^+$ $(0-{}^{13}C)$, arbitrarily chosen with an odd-even alternation and an abrupt drop beyond $x = 9$. For $x = 1, 2, 3, 4$, the abundance was set to zero. Panel (b) displays the ion yield Y_x calculated from Eq. (1) and plotted *versus* mass, i.e., a histogram of the mass spectrum that one would observe. The distinct isotope pattern of C_{70} appears below 845 u. $H_xC_{70}^+$ ions appear at 845 u and above; the abundance anomalies (i.e., the odd-even effect and the abrupt drop at $x = 9$, mass 849 u) are washed out significantly in the mass spectrum.

If the ion abundance shown in Figure 1(a) would apply to *deuterated* cluster ions $D_xC_{70}^+$ $(0-{}^{13}C)$, one would (with a straightforward modification of Eq. (1)) expect a mass spectrum as shown in Figure 1(c). The odd-even alternation and the abrupt drop beyond $x = 9$, mass 858 u, is much more recognizable in this spectrum. Experiments with deuterium are clearly preferable to experiments with hydrogen.

For the actual data analysis, one needs to invert the procedure, i.e., one determines the ion abundance from the measured ion yield. Equation (1) is a convolution of $A(x)$ with the function $P(x)$, thus one needs to deconvolute the measured ion yield. In the more general case, for example, in a measurement of $(CH_4)_xC_{70}^+$, the probabilities P_i will also depend on x and Eq. (1) is replaced by

$$Y_x = \sum P_{x,i} A_{x-i}. \tag{2}$$

This is a matrix equation, $Y = \boldsymbol{P}A$. One obtains the ion abundances from the inverse of the matrix, $A = \boldsymbol{P}^{-1}\ Y$. This is the method that we chose for data analysis with $\boldsymbol{P}^{-1}$ being replaced by the Moore-Penrose pseudoinverse.[35]

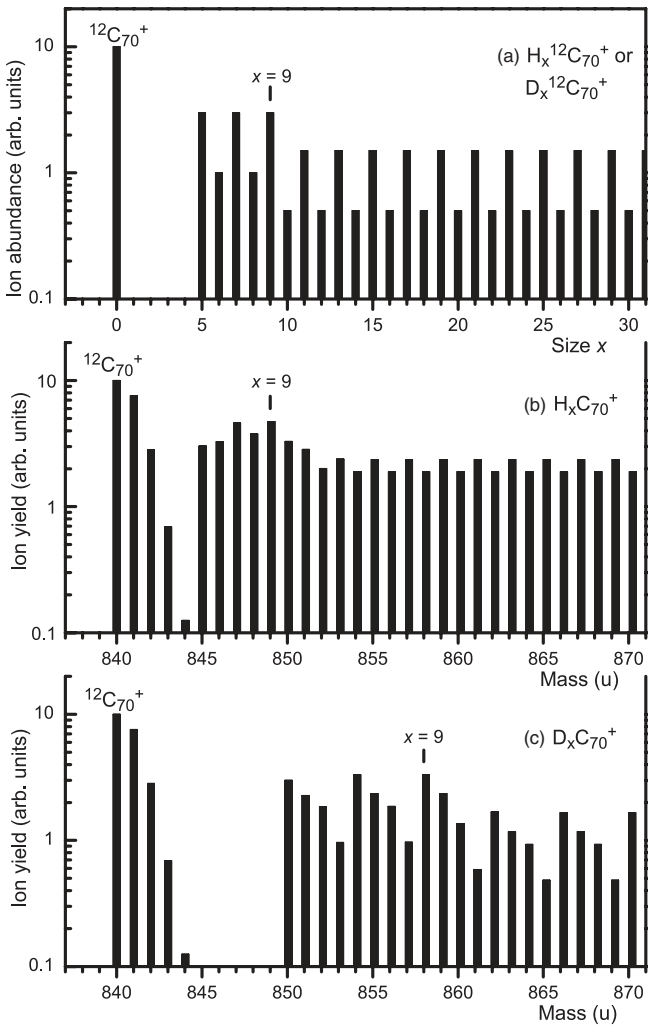

FIG. 1. Panel (a) An arbitrarily assumed distribution of isotopically pure $H_x{}^{12}C_{70}^+$ ions. From this ion *abundance* one computes the ion *yield*, i.e., the mass spectrum that one would measure (panel (b)). Panel (c) shows the simulated ion yield if, in panel (a), hydrogen were replaced with deuterium.

IV. THEORY

Energetics and geometries of neutral, singly and doubly charged $C_{60}H_x$ with x between 1 and 5 were calculated by means of density functional theory (DFT). Special attention was paid to the physisorption of one or two hydrogen molecules on C_{60}^+ or $C_{60}H^+$ ions. All structures were fully optimized in order to account for the deformation of the fullerene due to the presence of hydrogen. The calculations were performed with two different density functionals within the GAUSSIAN 09 program and a standard 6-31(d,p) basis set.[36] The PBE0 hybrid generalized gradient approximation functional from Adamo and Barone,[37] which is based on the pure functional of Perdew *et al.*[38] does not include long-range van der Waals interactions (dispersion).[39] It performs well, however, where static polarization[40] dominates and yielded good results for the singly charged systems. In order to include dispersion, the hybrid functional ωB97X-D[41] was used. This functional accounts empirically for long-range effects and has proven its suitability to describe weak interactions such as hydrogen bonds and dipole induced non-covalent bonds with good accuracy in many molecular systems.[42]

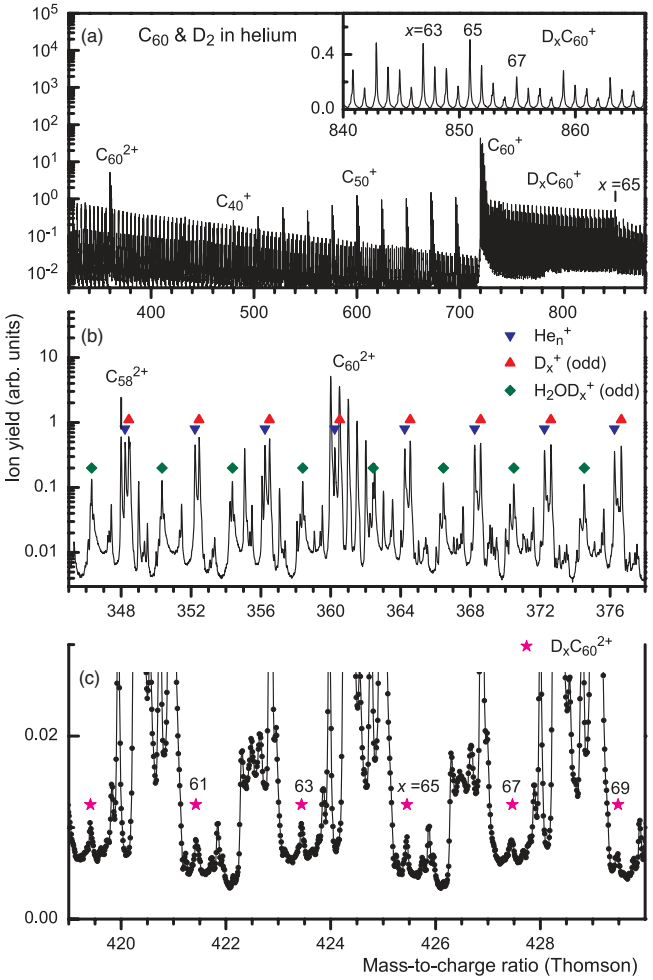

FIG. 2. Sections of a mass spectrum of helium droplets doped with C_{60} and D_2. Ions $D_xC_{60}^{z+}$ ($z = 1$ or 2) are labeled by the value of x. Note the anomaly in the ion yield of singly charged species at $x = 65$ in panel (a), the prominence of He_n^+ and D_x^+(x odd) in panel (b), and the appearance of doubly charged $D_xC_{60}^{2+}$ (panel (c)).

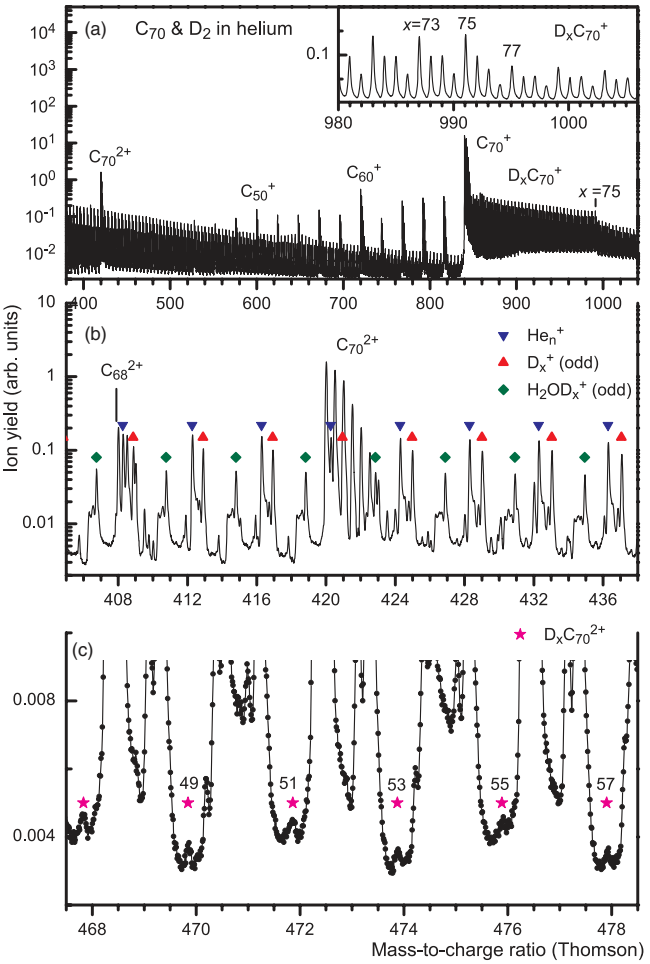

FIG. 3. Similar to Figure 2 for helium droplets doped with C_{70} and D_2; the anomaly occurs at $x = 75$ (see the inset in panel (a)).

V. EXPERIMENTAL RESULTS

A. Mass spectra

We have recorded several mass spectra of helium droplets doped with hydrogen or deuterium plus either C_{60} or C_{70}. Figure 2 displays sections of a spectrum obtained by electron ionization of droplets doped with C_{60} and D_2; Figure 3 displays sections of a spectrum of droplets doped with C_{70} and D_2. Two prominent ion series appear in these spectra below the fullerene mass, namely, He_n^+ and odd-numbered D_x^+. Each helium cluster ion He_n^+ gives rise to just one mass peak in the spectrum because helium is very nearly monoisotopic; the natural abundance of ^{4}He (mass 4.002603 u) is 99.999866%.[43] Similarly, each D_x^+ ion gives rise to one mass peak if one neglects the possible presence of H_2 impurities in the deuterium gas. In experiments carried out with H_2 instead of D_2, the presence of deuterium (natural abundance 0.0115%, mass 2.01410 u[43]) may be safely neglected. In the mass range displayed in Figs. 2(b) and 3(b), the mass of He_n^+ is about 0.3 u below that of D_{2n-1}^+. Even-numbered D_x^+ which have a yield of a few percent relative to adjacent odd-numbered D_x^+ [44] are overwhelmed in the current spectra by a series of impurity ions $H_2OD_x^+$ (x odd) which occurs 0.112 u below the D_x^+ (x even) series.

Other prominent ions in the low-mass section of the mass spectrum are singly charged fullerene fragments C_m^+ (m even) as small as C_{32}^+ in the C_{60} spectrum, and C_{36}^+ in the C_{70} spectrum. Doubly charged fullerenes C_{60}^{2+} and C_{70}^{2+} appear prominently at mass-to-charge ratios 360 and 420 Thomson, respectively; their even-numbered fragments C_m^{2+} can be identified down to C_{50}^{2+}. Each of these ions forms a characteristic pattern of peaks due to contributions from isotopologues that contain ^{13}C (natural abundance 1.07%, mass 13.003355 u). Most of these bare, singly or doubly charged C_m^{z+} ions ($z = 1$ or 2) probably result from direct ionization of bare C_{60} or C_{70} that leaks from the pickup cell into the ionizer. The intensity of these fragment ions relative to their doubly charged parent ions is greatly diminished in recent experiments with a modified setup that reduces the escape of fullerene vapor from the pickup cell.

The bottom panels in Figs. 2 and 3 reveal another, weak ion series which is assigned to odd-numbered doubly charged $D_xC_m^{2+}$ ($m = 60$ or 70). Because of interference with other ions, these ions can be unambiguously identified for only

one isotopologue, namely, $D_xC_{60}^{2+}$ ($0-^{13}C$) and $H_{x-1}C_{70}^{2+}$ ($1-^{13}C$) (i.e., $D_x{}^{12}C_{60}^{2+}$ and $H_{x-1}{}^{13}C^{12}C_{69}^{2+}$, respectively).

The top panels in Figs. 2 and 3 reveal an intense ion series of the form $D_xC_m^+$ ($m = 60$ or 70). The yield of these ion series drops abruptly beyond $x = 65$ and 75, respectively, as shown in more detail in the insets where mass peaks of odd-numbered, isotopically pure ($0-^{13}C$) ions are labeled by the value of x. The yield of even-numbered $D_xC_m^+$ (not labeled) is lower, but note that each mass peak contains contributions from several cluster ions. For example, the mass peak labeled $x = 73$ in Figure 3 contains contributions from $D_{73}C_{70}^+$ ($0-^{13}C$), some 30% from $D_{72}C_{70}^+$ ($2-^{13}C$), and a minor (≈1%) contribution from $D_{71}C_{70}^+$ ($4-^{13}C$). Similarly, the mass peak 1 u above the one labeled $x = 73$ is mostly due to $D_{73}C_{70}^+$ ($1-^{13}C$), but also contains contributions from $D_{72}C_{70}^+$ ($3-^{13}C$) and $D_{71}C_{70}^+$ ($5-^{13}C$). The analysis of the mass spectra, discussed in Sec. III, provides the *ion abundance,* which refers to specific, isotopically pure ions such as $D_xC_{70}^+$ ($0-^{13}C$).

B. Ion abundance

The ion abundance extracted from mass spectra recorded with D_2 is presented in Figure 4 for C_{60} and C_{70} (panels a and b, respectively), for singly charged odd-numbered, even-numbered, and doubly charged odd-numbered ions. Here, we have changed the notation for specifying the cluster size

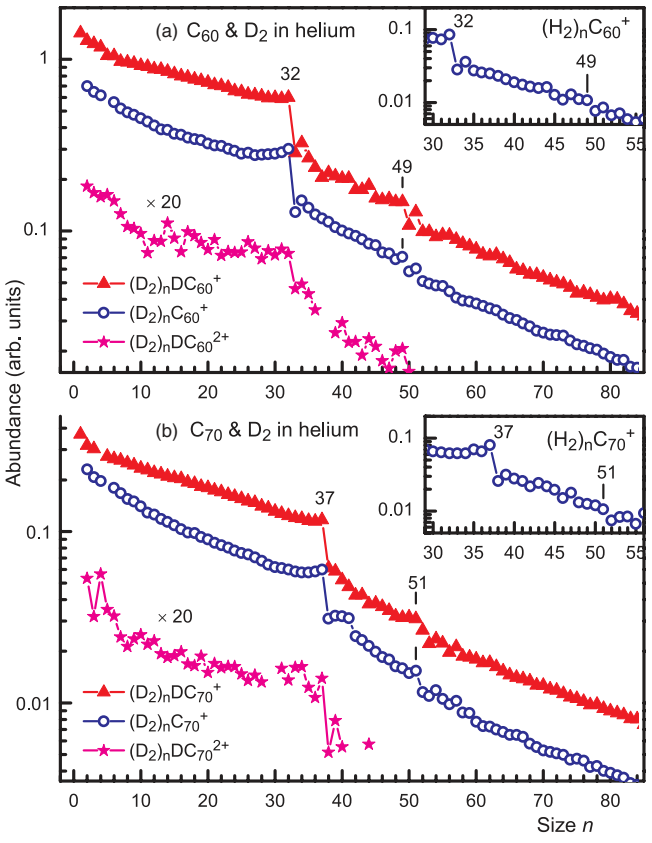

FIG. 4. Ion abundances of $(D_2)_nDC_m^+$, $(D_2)_nC_m^+$, and $(D_2)_nDC_m^{2+}$ extracted from mass spectra shown in Figs. 2 and 3 for $m = 60$ and 70, respectively. Significant anomalies in the ion abundance are marked. The insets display the ion abundances of $(H_2)_nC_{60}^+$ and $(H_2)_nC_{70}^+$.

to $(D_2)_nC_m^+$ and $(D_2)_nDC_m^+$ for even- and odd numbered $D_xC_m^+$, respectively.

The odd-numbered series is more abundant than the even-numbered series by about a factor two. For both ion series, the abundance varies very smoothly with size n until it drops abruptly by a factor two at (i.e., just beyond) $n = 32$ and 37 for C_{60} and C_{70}, respectively. Another drop occurs at $n = 49$ for C_{60} and 51 for C_{70}. These drops in abundance, by some 20%–30%, are significantly larger than the statistical uncertainty of the data points which is less than the size of the symbols. The same anomalies are observed in the ion abundance of $(H_2)_nC_{60}^+$ and $(H_2)_nC_{70}^+$ (see the insets in Figure 4) and $(H_2)_nHC_{60}^+$ and $(H_2)_nHC_{70}^+$ (not shown). In other words, there is no isotope effect in our data. The statistical significance of other, smaller anomalies seen in Figure 4 is questionable.

The abundance of doubly charged cluster ions in Figure 4 has been enhanced by a factor 20. Statistical scatter is large, but clear drops in the ion abundance occur at $n = 32$ and 37 for $(D_2)_nDC_{60}^{2+}$ and $(D_2)_nDC_{70}^{2+}$, respectively.

VI. RESULTS OF *AB INITIO* CALCULATIONS

In our previous work, covalent bonding of H and H_2 with C_{60}^+ was discussed.[12] Here, we consider the interaction of one to five hydrogen atoms with C_{60} with an emphasis on physisorption. The focus is on singly charged complexes to which the bulk of experimental data pertains, but for completeness we investigate some doubly charged and neutral complexes as well. The reaction energies are given in Table I for the functionals ωB97X-D (third column) and PBE0 (fourth column). These energies are obtained without zero-point correction. In the following discussion, we will refer to the ωB97X-D results unless explicitly mentioned otherwise. Some of the values of Table I are redundant since they can be calculated from other values of this table using the rows indicated in the comment column. For example, reaction 6 (3.2906 eV) plus reaction 11 (0.0732 eV) yields the energy of reaction 12 (3.3638 eV).

Comparing our values with the literature (references are provided in Table I) we find that both functionals (ωB97X-D and PBE0) perform remarkably well for the small molecules, reactions 2–4, and also for the ionization energy of the fullerene. Taking zero-point correction into account the bond energy of H_2 is 4.4533 eV (with ωB97X-D), close to the experimentally observed 4.4784 eV. The binding energy of H to C_{60}^+ (3.29 eV) obtained with ωB97X-D is 0.22 eV higher than the one obtained with PBE0. The H–C_{60} binding energy (2.16 eV) is in good agreement with a value reported by Vehvilainen *et al.*[45] who obtained 2.01 eV in a DFT calculation using the PBE functional and a plane wave basis set.

An energy barrier of 1.69 eV prevents chemisorption of H_2 at C_{60}^+ although the system with two covalent C–H bonds, $H_2C_{60}^+$, lies 1.50 eV below physisorbed $(H_2)C_{60}^+$ (in the following, H_2C_{60} will indicate two chemisorbed hydrogen atoms, while $(H_2)C_{60}$ indicates physisorbed dihydrogen). The energetically lowest isomer of $H_2C_{60}^+$ is the one labeled "1a,1b" in the study of neutral H_2C_{60} by Henderson *et al.*[46] Vehvilainen *et al.*[45] calculated a very large

TABLE I. Reaction energies ΔE. All values refer to the classical energy minima of reactants and products. H_2C_{60} indicates two chemisorbed hydrogen atoms while $(H_2)C_{60}$ indicates physisorbed dihydrogen.

Reaction Nos.	Reaction	ΔE (eV)[a]	ΔE (eV)[b]	Literature/comment
1	$C_{60} \rightarrow C_{60}^+ + e$	7.6469	7.3942	7.57,[c] 7.58[d]
2	$H_2 \rightarrow H_2^+ + e$	15.4849	15.3313	15.42593[e]
3	$H_2 \rightarrow 2H$	4.7304	4.5941	4.4784[e]
4	$H_3^+ \rightarrow H^+ + H_2$	4.5727	4.5524	4.377[e]
5	$HC_{60} \rightarrow H + C_{60}$	2.1630	2.1338	2.01[f]
6	$HC_{60}^+ \rightarrow H + C_{60}^+$	3.2906	3.0732	
7	$(H_2)C_{60} \rightarrow H_2 + C_{60}$	0.0495	0.0252	0.032,[g] 0.052[h]
8	$(H_2)C_{60}^+ \rightarrow H_2 + C_{60}^+$	0.0570	0.0376	
9	$H_2C_{60}^+ \rightarrow (H_2)C_{60}^+$	1.5001		
10	$(H_2)HC_{60}^+ \rightarrow H + (H_2)C_{60}^+$	3.3068	3.0652	From Reaction nos. 6, 8, and 11
11	$(H_2)HC_{60}^+ \rightarrow H_2 + HC_{60}^+$	0.0732	0.0297	
12	$(H_2)HC_{60}^+ \rightarrow H + H_2 + C_{60}^+$	3.3638	3.1029	From Reaction nos. 6 and 11
13	$(H_2)_2C_{60}^+ \rightarrow H + (H_2)HC_{60}^+$	1.4809	1.5564	From Reaction nos. 3, 10, and 14
14	$(H_2)_2C_{60}^+ \rightarrow H_2 + (H_2)C_{60}^+$	0.0573	0.0276	
15	$(H_2)_2C_{60}^+ \rightarrow 2H_2 + C_{60}^+$	0.1143	0.0652	From Reaction nos. 8 and 14
16	$(H_2)_2HC_{60}^+ \rightarrow H + (H_2)_2C_{60}^+$	3.3197	3.0636	From Reaction nos. 3, 13, and 17
17	$(H_2)_2HC_{60}^+ \rightarrow H_2 + (H_2)HC_{60}^+$	0.0702	0.0260	
18	$(H_2)_2HC_{60}^+ \rightarrow 2H_2 + HC_{60}^+$	0.1434	0.0557	From Reaction nos. 11 and 17
19	$(H_2)_2HC_{60}^+ \rightarrow H + 2H_2 + C_{60}^+$	3.4339	3.1288	From Reaction nos. 15 and 16
20	$(H_2)C_{60}^{2+} \rightarrow H_2 + C_{60}^{2+}$	0.0613		
21	$(H_2)H_2C_{60}^{2+} \rightarrow H_2 + H_2C_{60}^{2+}$	0.0845		
22	$(H_2)HC_{60}^{2+} \rightarrow H_2 + HC_{60}^{2+}$	0.0917		
23	$H_2 + C_{60}^{2+} \rightarrow H + HC_{60}^{2+}$	1.3100		
24	$(H_2)_2 + C_{60}^{2+} \rightarrow H + (H_2)HC_{60}^{2+}$	1.2183		
25	$H_2C_{60}^{2+} \rightarrow (H_2)C_{60}^{2+}$	1.8483		
26	$(H_2)H_2C_{60}^{2+} \rightarrow (H_2)_2C_{60}^{2+}$	1.8733		

[a] ωB97X-D without zero-point correction and without CP correction.
[b] PBE0 without zero-point correction and without CP correction.
[c] Reference 63.
[d] Reference 85.
[e] Reference 86.
[f] Reference 45.
[g] Reference 47.
[h] Reference 48.

barrier of 3.7 eV between the physi- and chemisorbed states of the neutral system and an exothermicity of only 0.6 eV for chemisorption.

Next, the physisorbed systems $(H_2)C_{60}$ and $(H_2)C_{60}^+$ will be discussed. The calculated adsorption energies are 49.5 and 57 meV, respectively. As expected, smaller energies result from the PBE0 functional, e.g., 38 meV instead of 57 meV for $(H_2)C_{60}^+$. As already pointed out by Yoon *et al.*,[6] charged fullerenes bind H_2 more strongly than neutral C_{60}. Physisorption of H_2 on neutral fullerenes has already been investigated by Korona *et al.*[47] using symmetry adapted perturbation theory, and by Denis[48] using local spin density approximation (LSDA) including the counterpoise correction (CP). Korona *et al.*[47] obtained 32 meV at a distance of 6.5 Å from the center of C_{60}, while Denis[48] reports an adsorption energy of 52 meV without mentioning details of the optimized geometry. The values are in very good agreement with our values of 49.5 meV (at 6.2 Å) without CP or 37.5 meV (at 6.2 Å) including CP; i.e., the CP correction amounts to 12 meV. Thus, we estimate that counterpoise corrected values for adsorption energies listed in Table I would be approximately 10 meV lower, but the trends are correct nevertheless and the CP correction often overshoots.

Also of interest is a comparison with data for physisorption of H_2 on nanotubes and graphene. From a Raman study of H_2 adsorbed on single-walled nanotubes, Williams *et al.*[49] estimate a well depth of 46.6 meV; the molecule is preferentially oriented flat against the surface. Brown *et al.*,[50] based on inelastic neutron scattering data, estimate a desorption energy of about 62 meV for single-walled nanotubes. Alonso and co-workers have calculated the interaction of H and H_2 with single-walled nanotubes.[51] Their results depend on the type of tube ((5,5) and (6,6) tubes have been considered), and whether or not the carbon atoms are allowed to relax; H_2 is bound to the outside of the tubes by 40–70 meV. In later work they reported binding energies up to 100 meV for other types of nanotubes.[52] For graphene, calculated binding energies range from about 56 to 86 meV.[53] It is reasonable that our result for C_{60} is less than values for single-walled nanotubes and graphene because of the stronger curvature of the C_{60}.[45,54]

In order to estimate the influence of zero-point vibrations on the physisorption energies the potential energy curve for $(H_2)C_{60}^+$ was calculated; it is depicted in Figure 5 together with its five bound vibrational levels that are eigenstates to the radial Schrödinger equation with reduced mass 3664.5 a.u.

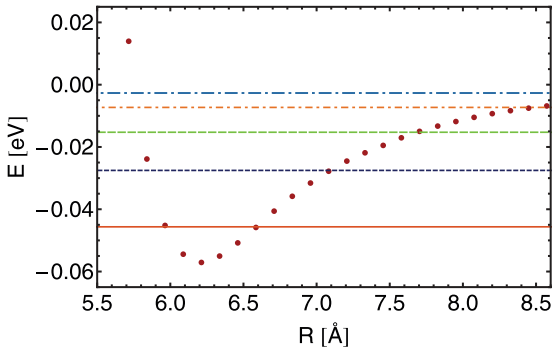

FIG. 5. Potential energy of physisorbed $(H_2)C_{60}^+$. Considered as a two body potential it supports five vibrational levels at −0.046 eV (solid line), −0.028 eV, −0.0015 eV, −0.007 eV, and −0.003 eV.

With this approximation for the zero-point energy (which neglects all other possible vibrational degrees of freedom) the physisorption energy is reduced from 57 to 46 meV.

Under our experimental conditions, the probability for a hydrogen molecule to overcome the large barrier of 1.69 eV to covalently bind to C_{60}^+ is exceedingly low. A reaction with H_3^+, however, faces no barrier at all. The proton affinity of C_{60} (9.27 eV) is large enough to cause an immediate reaction with H_3^+ to an equilibrium geometry where one H binds covalently to C_{60}, now positively charged, and H_2 is physisorbed. The overall process does not differ much from a sequential reaction of H^+ and H_2 with C_{60}. The physisorbed H_2 remains at 3.3–3.4 Å (PBE0) or 2.94–3.03 Å (ωB97X-D) away from a face of the fullerene. This distance varies slightly due to two effects. First, it depends on the position of the hydrogen molecule with respect to the position of the covalently bound H atom. Second, there are different local minima in the potential surface over hexagons or pentagons. The most stable structure obtained for $(H_2)HC_{60}^+$ is shown in Figure 6(a). H_2 is positioned over the hexagon which is closest to the covalently bound hydrogen atom, parallel to the hexagonal face. The total energy of this configuration lies 4.77 eV below the energy of separated H_3^+ and C_{60}. The physisorption energy of H_2 is 73 meV for this configuration; a smaller value of 66 meV is obtained for H_2 over the pentagon adjacent to the covalently bound H (see Table II). On the other hand, if H_2 attaches to C_{60}^+ over a hexagonal face far away from C–H (Figure 6(b)), the binding energy decreases to 58 meV, nearly the same as the 57 meV of H_2 interacting with pristine C_{60}^+. In other words, the bound H facilitates the physisorption of H_2 in its vicinity.

Analysis of the site dependence has been extended to systems with two H_2 molecules physisorbed at C_{60}^+. Energies are listed in Table II; optimized structures are shown in Figs. 6(c)–6(e). In general, hexagonal faces are energetically preferred to pentagonal faces by about 10 meV. Second, clustering of the adsorbate increases the adsorption energy, as already observed for $(H_2)HC_{60}^+$. For $(H_2)_2C_{60}^+$, the energy to remove one H_2 is 57 meV, the same as for $(H_2)C_{60}^+$ if the two H_2 are adsorbed over adjacent hexagons; the adsorption energy decreases to 48 meV if the two H_2 are adsorbed over opposite hexagons.

Results for doubly charged cations are compiled in Table I. The physisorption energy of H_2 on C_{60}^{2+} of 61.3 meV is, not surprisingly, slightly higher than the value for singly charged fullerenes (57 meV); Yoon *et al.* reported an even stronger increase by about 0.015 eV.[6] The physisorption energy of H_2 on HC_{60}^{2+} (91.7 meV) is, as expected, larger than for H_2 on pristine C_{60}^{2+} and also larger than on singly charged HC_{60}^+ (73.2 meV). The physisorption energies on HC_{60}^+ and HC_{60}^{2+} are higher than on C_{60}^+ and C_{60}^{2+}, respectively, but a second chemisorbed H does not increase the physisorption energy any further; see reactions 21 and 22.

Another interesting aspect is reaction 23 in which a free H_2 is converted to a chemisorbed H plus a free H. The reaction is endothermic by 1.30 eV if it involves C_{60}^{2+}. The endothermicity of H production decreases by 0.09 eV if the reagent is replaced by $(H_2)_2$ (reaction 24). However, it is questionable if reaction of a large hydrogen cluster with C_{60}^{2+} could possibly produce atomic hydrogen. We also note that the energy difference between chemisorbed and physisorbed H_2 of the doubly charged complex is larger by 0.35 eV than for the singly charged complex (reactions 9 and 25).

TABLE II. Adsorption energies and distance from the center of the fullerene to the center of H_2 for various structures and positions (without zero-point correction, computed with ωB97X-D). "Adjacent" and "opposite" positions are relative to other hydrogen; some structures are illustrated in Figure 6.

Reaction	Position	Energy (eV)	Distance (Å)	Fig. 6
$(H_2)C_{60} \rightarrow H_2 + C_{60}$	Hex	0.0495	6.178	
	Pent	0.0388	6.368	
$(H_2)C_{60}^+ \rightarrow H_2 + C_{60}^+$	Hex	0.0570	6.213	
	Pent	0.0445	6.394	
$(H_2)HC_{60}^+ \rightarrow H_2 + HC_{60}^+$	Hex adj	0.0732	6.192	(a)
	Pent adj	0.0659	6.385	
	Hex opp	0.0581	6.193	(b)
$(H_2)_2C_{60}^+ \rightarrow H_2 + (H_2)C_{60}^+$	Hex and hex adj	0.0573	6.206 and 6.209	(c)
	Hex and pent adj	0.0452	6.211 and 6.386	
	Hex and hex opp	0.0477	6.202 and 6.202	(d)
$(H_2)_2HC_{60}^+ \rightarrow H_2 + (H_2)HC_{60}^+$	Hex and hex adj	0.0702	6.184 and 6.194	
	Hex and pent adj	0.0641	6.183 and 6.373	(e)

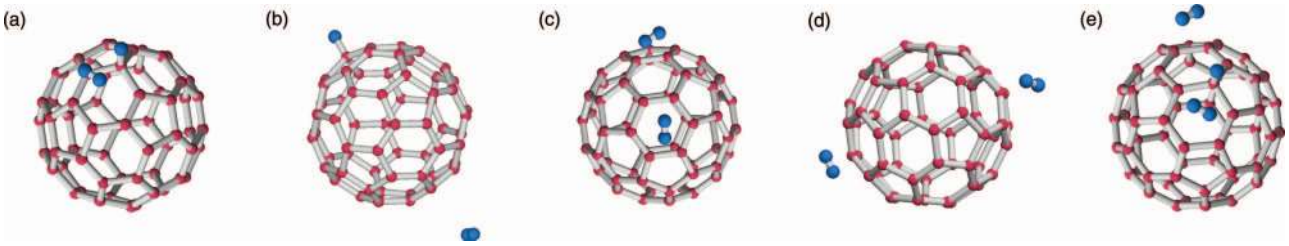

FIG. 6. Five different optimized $H_xC_{60}^+$ structures: $(H_2)HC_{60}^+$ ((a) and (b)), $(H_2)_2C_{60}^+$ ((c) and (d)), $(H_2)_2HC_{60}^+$ (e).

VII. DISCUSSION

Two singly charged ion series have been identified in mass spectra of helium nanodroplets doped with fullerene and hydrogen, namely, odd-numbered $H_xC_m^+$ (x odd, also written $(H_2)_nHC_m^+$), and even-numbered $H_xC_m^+$ (written $(H_2)_nC_m^+$), where $m = 60$ or 70. In experiments with D_2 the corresponding ion series have been identified, plus doubly charged odd-numbered $(D_2)_nDC_m^{2+}$. We have not found any statistically significant differences in the ion abundance of fullerenes complexed with H_2 and D_2 but anomalies in the ion abundance are more reliably extracted from experiments with D_2 because the presence of isotopologues that contain one or more ^{13}C tends to wash out anomalies in the mass spectra as illustrated in Figure 1. In the following discussion, which will focus mostly on singly charged species, the term "hydrogen" or H_2 will refer to the element; we will not distinguish between H_2 and D_2 except when specifically looking for a H–D isotope effect.

A. Ionization mechanism and the odd-even effect

Ionization of pure hydrogen clusters by electron impact or UV photons primarily results in odd-numbered cluster ions $[(H_2)_nH]^+$; the abundance of even-numbered $(H_2)_n^+$ is lower by about two orders of magnitude.[55] The low intensity of $(H_2)_n^+$ arises from the large exothermicity of the reaction

$$H_2^+ + H_2 \rightarrow H_3^+ + H + 1.727\,\text{eV}; \qquad \text{(R1)}$$

the exothermicity follows from the H_2^+ bond strength of 2.650 eV[56] and the H_2 proton affinity of 4.377 eV (Table I). The hydrogen dimer $(H_2)_2$ is very weakly bound; therefore, a similarly large reaction energy is released after vertical ionization of $(H_2)_2$. According to an *ab initio* direct dynamics calculation, vertical ionization of the H_2 dimer, trimer, or hexamer leads to rapid formation of a vibrationally hot H_3^+ and ejection of an energetic hydrogen atom even though H_3^+H is intrinsically stable with respect to H loss.[57]

Electron ionization of hydrogen clusters embedded in helium nanodroplets (in the absence of C_{60}) also results in predominantly odd-numbered hydrogen cluster ions[44,58] even though the ionization mechanism is very different, namely, charge transfer from helium cations[15,59,60] *versus* direct ionization (details of the ionization mechanism will be discussed in Sec. VII B). Thus, the strong suppression of the odd-even effect for $H_xC_m^+$ cluster ions must be sought in the role of the fullerene.

Successive pickup of molecules by a helium nanodroplet will always lead to growth of a single cluster ($(H_2)_nC_{60}$ in the present study) in the center of the superfluid droplet[33] unless the pickup rate is extremely large.[62] Thus, one has to consider reactions following charge transfer from He^+ directly to C_{60} (ionization energy 7.57 eV[63]), or via the hydrogen layer to C_{60}. We first consider the energetics of $(H_2)_nC_{60}$. The data in Table I reveal that ejection of H from $(H_2)_2C_{60}^+$ (with H_2 being physisorbed) is significantly endothermic,

$$(H_2)_2C_{60}^+ \rightarrow (H_2)HC_{60}^+ + H - 1.48\,\text{eV}. \qquad \text{(R2)}$$

Even more importantly, the reaction is impeded by a large energy barrier. For reaction (R2) to take place one of the physisorbed H_2 molecules has to overcome a barrier of 1.69 eV (computed for $H_2C_{60}^+$) that separates the physisorbed from the chemisorbed species. Thus, if ionization of the hydrogen-fullerene complex occurs by direct charge transfer from He^+ to C_{60}, ejection of H and the formation of odd-numbered $(H_2)_nHC_{60}^+$ would be suppressed.

On the other hand, if the fullerene were initially fully coated by layers of H_2 one may expect charge transfer to the hydrogen layer and formation of H_3^+ because of the large exothermicity of reaction (R1) which is barrierless;[57] H would be rapidly expelled before the net charge is eventually transferred to the fullerene.

The fact that we observe approximately equal (within a factor two) abundances for odd- and even-numbered $H_xC_m^+$ suggests that both scenarios, direct or indirect charge transfer from He^+ to C_{60}, apply. Testing this proposition would be difficult, though. The number of H_2 in the initial neutral complex will always feature a broad distribution, and charge transfer from He^+ to the dopant will release a very large amount of energy (about 18 eV, the difference between the ionization energies of He and C_{60}). As a result, a large number of H_2 (in addition to He) will be ejected from the nascent ion, and the neutral precursors of the observed $H_xC_m^+$ ions will be complexes containing a large, poorly defined number of H_2. It would, therefore, be difficult to observe a correlation between the average number of H_2 in the neutral complex (controlled by the H_2 pressure in the pickup cell), and the relative abundance of even-numbered $(H_2)_nC_m^+$.

B. Doubly charged ions

A weak series of doubly charged $[(H_2)_nHC_m]^{2+}$ is observed in Figs. 2 and 3. The ions could be identified only when deuterium was used, and only for one particular isotopologue

of the fullerene. The appearance of these ions is remarkable for two reasons:

(1) The observed doubly charged complexes $[(H_2)_nHC_m]^{2+}$ are surprisingly small, even $[(H_2)HC_m]^{2+}$ is identified, and
(2) The formation of doubly charged complexes upon electron ionization of doped helium clusters is rather uncommon.[64]

First, homogeneous van der Waals bound clusters are not observable below a size limit, or "critical size" because of spontaneous charge separation (Coulomb explosion) into singly charged fragments. No doubly charged pure hydrogen cluster ions have yet been reported; a simple model that is based on a liquid-drop approximation predicts a critical size of $n = 863$ for $(H_2)_n^{2+}$.[65] Second, when helium droplets doped with a complex X interact with energetic electrons, the probability of direct ionization of X is vanishingly small. Instead, either He^+ or a metastable He^* ($2\,^3S_1$) are formed, with energy thresholds of 24.59 and 19.8 eV, respectively. Rapid motion of He^+ towards the dopant, followed by charge transfer,

$$He^+ + X \rightarrow He + X^+ \tag{R3}$$

proceeds by charge hopping aided by the attraction between the ion and the induced-dipole moment of the dopant.[15,59] If X is a molecule or cluster it may fragment further, $X^+ = (AB)^+ \rightarrow A^+ + B$.

Alternatively, ionization of the dopant may proceed by Penning ionization,

$$He^*(2\,^3S_1) + X \rightarrow He + X^+ + e. \tag{R4}$$

Penning ionization is particularly efficient when the dopant resides on the surface,[61] but there is experimental evidence that it is also relevant for the formation of doubly charged dopant ions.[64]

A doubly charged dopant can be formed only if its ionization energy is below the energy to form $He^*(2\,^3S_1)$ or He^+. This condition is rarely met for chemically stable molecules. The energy required to form $2H^+$ from H_2, 31.7 eV, is readily computed from the data in Table I. However, the energies required to form C_{60}^{2+} or C_{70}^{2+} from the respective neutral precursors are only 19.00 and 18.84 eV, respectively.[66] Therefore, a doubly charged fullerene with one or more hydrogen attached could be formed by either Penning ionization or charge transfer from He^+. For example, consider the energetics of $[H_2C_{60}]^{2+}$:

$$H_2C_{60} \rightarrow H_2 + C_{60} - 0.050\,\text{eV}, \tag{R5a}$$

$$\rightarrow H_2^+ + C_{60}^+ + 2e - 23.05\,\text{eV}, \tag{R5b}$$

$$\rightarrow H_2 + C_{60}^{2+} + 2e - 19.05\,\text{eV}, \tag{R5c}$$

where the reaction energies are computed from entries in Table I (using experimental values if available), and the energy required to form C_{60}^{2+} from C_{60}.[66] Reaction (R5c) is less endothermic than the charge separation reaction (R5b) by 4.0 eV. As a result one expects that the two positive holes in the complex $[H_2C_{60}]^{2+}$ are localized on the fullerene, H_2 is physisorbed at C_{60}^{2+}, and $H_2C_{60}^{2+}$ is stable with respect to charge separation. A similar reasoning explains why small doubly charged cluster ions such as He_nPb^{2+}, formed by ionization of lead-doped helium droplets with a femtosecond laser, or $(CO_2)_nCu^{2+}$ formed by electron ionization of neutral clusters,[67] are stable with respect to charge separation for all values of n.

The energetics of odd-numbered $[(H_2)_nHC_m]^{2+}$ will be different but here, too, the two holes are likely to be localized on the fullerene. The energetics also depend on the ligand. In our previous work on water-C_{60} and ammonia-C_{60} complexes, we had observed dehydrogenated ions, $(H_2O)_nOHC_{60}^+$ and $(NH_3)_nNH_2C_{60}^+$ which were particularly prominent for $n = 0$.[68] We hypothesized that they involve an intermediate C_{60}^{2+} followed by charge transfer to the ligands and charge separation into dehydrogenated plus protonated ions. For water, the first ionization energy (12.621 eV) is close to the second ionization energy of C_{60} (11.4 eV) and for NH_3 the first ionization energy (10.070 eV) is even lower; this provides a rational for the absence of doubly charged ions in those studies.

The picture presented so far is incomplete. First, another mechanism that may occur at high electron energies (70 eV were used in the current study) is formation of two He^* within the same droplet by the incident electron; sequential Penning ionization will then provide a total energy of 2×19.8 eV. An energy threshold of 40 eV was, indeed, observed for the formation of doubly charged fragment ions of CH_3I.[64] In another recent study, methane clusters in helium were ionized by electron ionization; doubly charged $(CH_4)_n^{2+}$ were observed above a critical size of 70 with an energy threshold of 44 eV.[69] The findings were attributed to formation of $He^*(2\,^3S_1) + He^+$. In this model, a singly charged dopant ion is formed by charge transfer from He^+; Penning ionization of the ion in a collision with He^* is then facilitated by the large attraction between the dopant ion and the highly polarizable He^*.[69]

The very weak signal of doubly charged ions in the present study precludes a measurement of their appearance energy; their formation may be due to any one of the four mechanisms mentioned above, or a combination of them: Penning ionization with He^*, charge transfer from He^+, sequential Penning ionization, or charge transfer followed by Penning ionization. All these processes would be energetically feasible.

C. Abundance anomalies and adsorption of H_2 on graphitic surfaces

The ion abundance was extracted from the ion yield measured by mass spectrometry as described in Sec. III, in order to correct for contributions of isotopologues containing one or more ^{13}C.

Anomalies in the abundance A_n of cluster ions may be caused by several factors including kinetics, size-selective ionization or detection, etc. For atomic clusters that are prone to fragmentation upon ionization, including

van-der-Waals clusters embedded in helium,[70] the most likely cause are anomalies in the dissociation energies D_n (often called evaporation or separation energies), i.e., the difference between total energies E_n of cluster ions of adjacent size in their most stable configurations,

$$D_n = -E_n + E_{n-1}. \tag{3}$$

The relation between the size dependence of D_n and A_n has been explored by several authors,[71] based on the model of the evaporative ensemble.[72] Key ingredients of this model are that the initial cluster distribution is broad, dissociation is a statistical process, and each cluster ion that is observed has undergone at least one evaporation. The small heat capacity of clusters containing less than $n \approx 10^2$ units ensures that each evaporation cools the cluster significantly, thus leading to a drastic (at least a factor 10) reduction of the rate coefficient k. As a result, an ion ensemble that is interrogated at some time t after ionization will be characterized by rather well defined upper and lower limits to its (vibrational) excitation energy $E_n{}^*$.[73] The energy limits are related to the dissociation energies D_n and D_{n+1}, respectively. An upper limit exists because very hot $X_n{}^+$ would rapidly dissociate into $X_{n-1}{}^+$; a lower limit exists because very cold precursor ions $X_{n+1}{}^+$ will not dissociate into $X_n{}^+$ on the experimental time scale. The energy limits depend only weakly on the time t through the Gspann factor, $G = \ln(t\nu)$,[72,74] where ν is the frequency factor in the Arrhenius relation,

$$k = \nu \exp\left(-\frac{D_n}{k_B T_e}\right), \tag{4}$$

Here, k_B is the Boltzmann factor, and T_e is the emission temperature.[75] If the microcanonical heat capacities C_n of the cluster ions are approximated by the equipartition theorem, $C_n = (3n - 7)k_B$, one can derive a quantitative relation between relative dissociation energies $D_n/\widetilde{D_n}$ and relative ion abundances $A_n/\widetilde{A_n}$, where the tilded quantities are functions that are obtained by fitting smooth functions to D_n and A_n, respectively.[76] Normalization to these smooth functions is needed because local anomalies in the ion abundance provide information about local variations in D_n, not about global trends.

A special situation arises if C_n is much less than the classical value, a situation probably encountered for alkali monomer and dimer ions solvated in helium,[77] and fullerene ions solvated in helium[10] or hydrogen. The computed energies for desorption of H_2 from $H_xC_{60}{}^+$ ($x = 2, 3, 4, 5$) amount to 50–70 meV (Table I); the corresponding vibrational temperature of the complexes may thus be estimated from the evaporative model to be 30–40 K.[78,79] At this temperature $C_{60}{}^+$ will be in its vibrational ground state, and one obtains the simple relation

$$D_n = \frac{A_n}{\widetilde{A_n}}\widetilde{D_n}, \tag{5}$$

that is, local variations in the abundance are directly proportional to local variations in the dissociation energy. Additional details have been discussed in Ref. 77.

We have applied Eq. (5) to derive relative dissociation energies $D_n/\widetilde{D_n}$ of singly charged hydrogen-fullerene complexes; results are displayed in Figure 7. The smooth functions $\widetilde{A_n}$ were obtained from the ion abundances (Figure 4) by weighted averaging over several adjacent sizes.[76] The weights were calculated from a Gaussian with a fixed width of $\Delta n = 2$ (standard deviation). The procedure reveals that the main anomalies translate to a local enhancement of the dissociation energy by 30%–50% for the most stable cluster (at $n = 32$ for C_{60} and 37 for C_{70}), and a decrease by some 30% relative to the average energy for $n = 33$ and 38, respectively. These values do not change much if the smooth function $\widetilde{A_n}$ is derived differently.

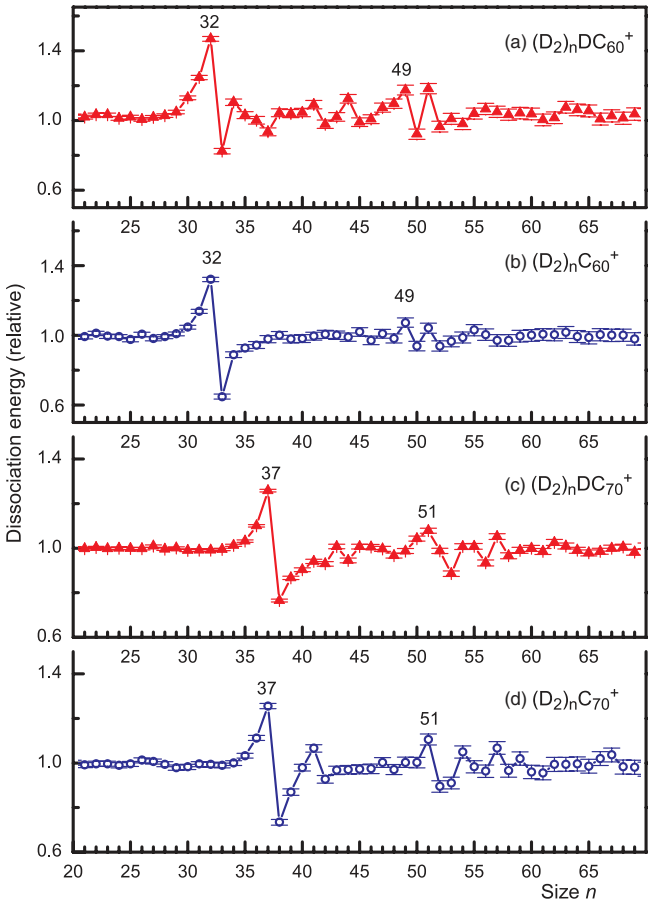

FIG. 7. Relative dissociation energies derived from the ion abundance (Figure 4) with the help of Eq. (5).

An appealing interpretation of the abundance anomalies of even-numbered hydrogen-fullerene complexes $(H_2)_nC_m{}^+$ is an enhanced ion stability when one H_2 is bound to each of the carbon rings of the fullerene substrate. Fullerenes are characterized by 12 pentagons; the number of hexagonal faces is 20 for C_{60} and 25 for C_{70}. The corresponding anomalies at 32 and 37 have also been observed for complexes of fullerenes with alkaline earth metals,[80] helium,[10] and methane.[81] This interpretation would also provide a rational for the abundance anomalies observed for the odd-numbered series $(H_2)_nHC_m{}^{z+}$ at 32 ($m = 60$) and 37 ($m = 70$), for $z = 1$ and 2, because our calculations indicate that the additional lone H atom would be covalently bound atop a carbon atom; it would not block any of the adsorption sites over the hexagons or pentagons that are preferred by the physisorbed H_2 molecules.

A fully decorated fullerene may be viewed as the analogue of a graphite surface, or graphene sheet, with the adsorbate forming the commensurate 1 × 1 phase on the honeycomb lattice. This phase does not actually form because it would imply a separation of only 2.46 Å between adjacent adsorbate molecules, significantly less than the size of H_2 or He. At lower coverage, however, a commensurate adsorbate layer forms in which all second-nearest hexagonal adsorption sites are occupied. The density of this so-called $\sqrt{3}\times\sqrt{3}$ commensurate phase is 0.0637 $Å^{-2}$, one third of the 1 × 1 phase; the spacing between adsorbate molecules is $2.46\sqrt{3} = 4.26$ Å.

However, the nearest-neighbor distance in crystalline hydrogen is only 3.75 Å.[82] Thus, the $\sqrt{3}\times\sqrt{3}$ commensurate phase is underdense; the first monolayer of H_2 on graphite is not complete until the coverage reaches 0.0927 $Å^{-2}$.[9] Might the commensurate 1 × 1 phase of H_2 on C_{60}^+ formed at $n = 32$ be underdense as well? In recent theoretical studies of neutral or cationic He_nC_{60}, it was found[10,11,83] that the first solvation shell can accommodate many more atoms in addition to 32 that are in registered sites, in agreement with experiment.[10] Similar theoretical studies are not available for the hydrogen-C_{60}^+ system but if one multiplies the number (60) of atoms in the first solvation shell of helium-C_{60}^+ with the ratio between the monolayer coverage of H_2 on graphite (0.0927 $Å^{-2}$)[9] and He on graphite (0.120 $Å^{-2}$)[84] one expects that $(H_2)_nC_{60}^+$ can accommodate ≈46 H_2 in its first solvation shell. Similarly, for $He_nC_{70}^+$ we observed closure of the first solvation shell at 62;[10] scaled as described above one predicts that $(H_2)_nC_{70}^+$ completes the first solvation shell at ≈48. These values (46 and 48) agree quite well with the anomalies observed at $n = 49$ and 51, see Figure 7. Thus, these values signal the closure of the first H_2 solvation shells around C_{60}^+ and C_{70}^+.

The hydrogen -graphite system shows a pronounced isotope effect: The density of the first deuterium monolayer is 0.0987 $Å^{-2}$, 6.5% larger than for H_2.[9] A similarly large isotope effect for the hydrogen-fullerene system would increase the number of molecules in the first solvation shell from 49 to 52 for C_{60}^+, and 51 to 54 for C_{70}^+. No such shift is seen in the experimental data. The isotope effect on graphene stems from the larger delocalization of the lighter H_2 molecules, leading to an increased repulsion at a given distance, compared to D_2. One may speculate that the increased binding between hydrogen or deuterium and charged fullerenes, as opposed to the weaker binding with planar graphite, mitigates the isotope effect. Another factor may be the corrugation which is stronger over the curved fullerene surface, thus hindering the addition of hydrogen molecules beyond the 1 × 1 phase. A third and more compelling reason for the lack of an isotope effect for fullerenes might be that, for a curved substrate, the H_2 molecules can reduce their mutual repulsion by filling the solvation shell at a slightly larger distance from the center of C_{60}^+ if this is energetically more favorable than lowering the solvation number. We cannot compute the effect of zero point motion for a fully solvated C_{60}^+, but for $(H_2)C_{60}^+$ we find that the mean radial distance in the quantum mechanical ground state is, indeed, about 0.55% larger than for $(D_2)C_{60}^+$. Obviously such an increase in distance would not mitigate the repulsion between neighbors over a planar substrate.

VIII. CONCLUSIONS

The corrugation of graphitic surfaces is known to affect the phase diagram of adsorbates. The strength of the corrugation may be increased, for example, by increasing the curvature of the surface. At the same time, curvature also increases the distance between molecules that reside in commensurate adsorption sites. The curvature of the C_{60} surface is large enough to accommodate one hydrogen molecule per polygon in an energetically preferred phase that is equivalent to the 1 × 1 phase which is not accessible to H_2, He, or other gases over a planar graphitic surface. The commensurate 1 × 1 phase is also observed for C_{70} cations, and doubly charged C_{60} and C_{70}. Furthermore, our data suggest that the first adsorption layer is not complete until 17 additional H_2 molecules are adsorbed on C_{60}^+, or 14 on C_{70}^+. C_{70}^+ shows a smaller increase because the average curvature and thus the average distance between H_2 adsorbed in the commensurate phase is smaller than for C_{60}. Although our experimental approach has its shortcomings, e.g., we cannot control the temperature, it does provide accurate values for the coverage and, hence, allows to accurately determine the effect of curvature on adsorption.

ACKNOWLEDGMENTS

C.L. and P.B. acknowledge a dissertation grant from the vicerectorate for research of the University of Innsbruck. This work was supported by the Austrian Science Fund, Wien (FWF, Project Nos. P19073, L633, and J2973-N20). Part of this work was supported by the Austrian Ministry of Science BMWF as part of the UniInfrastrukturprogramm of the Research Platform Scientific Computing at the University of Innsbruck and was funded by the Austrian Science Fund (FWF) DK+ project Computational Interdisciplinary Modeling, W1227.

[1] G. W. Crabtree and M. S. Dresselhaus, MRS Bull. **33**, 421 (2008).
[2] L. Schlapbach and A. Züttel, Nature (London) **414**, 353 (2001).
[3] U.S. Department of Energy, Energy Efficiency and Renewable Energy/Hydrogen Storage, see http://www1.eere.energy.gov/hydrogenandfuelcells/storage/current_technology.html, 2013.
[4] H. Furukawa and O. M. Yaghi, J. Am. Chem. Soc. **131**, 8875 (2009); H. Furukawa, N. Ko, Y. B. Go, N. Aratani, S. B. Choi, E. Choi, A. O. Yazaydin, R. Q. Snurr, M. O'Keeffe, J. Kim, and O. M. Yaghi, Science **329**, 424 (2010); P. B. Sorokin, H. Lee, L. Y. Antipina, A. K. Singh, and B. I. Yakobson, Nano Lett. **11**, 2660 (2011); P. Jena, J. Phys. Chem. Lett. **2**, 206 (2011); N. Park, K. Choi, J. Hwang, D. W. Kim, D. O. Kim, and J. Ihm, Proc. Natl. Acad. Sci. U.S.A. **109**, 19893 (2012).
[5] A. C. Dillon, K. M. Jones, T. A. Bekkedahl, C. H. Kiang, D. S. Bethune, and M. J. Heben, Nature (London) **386**, 377 (1997); Y. Ye, C. C. Ahn, C. Witham, B. Fultz, J. Liu, A. G. Rinzler, D. Colbert, K. A. Smith, and R. E. Smalley, Appl. Phys. Lett. **74**, 2307 (1999); M. Yoon, S. Y. Yang, C. Hicke, E. Wang, D. Geohegan, and Z. Y. Zhang, Phys. Rev. Lett. **100**, 206806 (2008); K. R. S. Chandrakumar and S. K. Ghosh, Nano Lett. **8**, 13 (2008); D. Saha and S. G. Deng, Carbon **48**, 3471 (2010); Y. Yamada, Y. Satake, K. Watanabe, Y. Yokoyama, R. Okada, and M. Sasaki, Phys. Rev. B **84**, 235425 (2011); P. Mauron, A. Remhof, A. Bliersbach, A. Borgschulte, A. Zuttel, D. Sheptyakov, M. Gaboardi, M. Choucair, D. Pontiroli, M. Aramini, A. Gorreri, and M. Ricco, Int. J. Hydrogen Energy **37**, 14307 (2012).
[6] M. Yoon, S. Y. Yang, E. Wang, and Z. Y. Zhang, Nano Lett. **7**, 2578 (2007).

[7]M. Bienfait, P. Zeppenfeld, N. Dupont-Pavlovsky, M. Muris, M. R. Johnson, T. Wilson, M. DePies, and O. E. Vilches, Phys. Rev. B **70**, 035410 (2004).
[8]H. Freimuth, H. Wiechert, and H. J. Lauter, Surf. Sci. **189**, 548 (1987).
[9]H. Freimuth, H. Wiechert, H. P. Schildberg, and H. J. Lauter, Phys. Rev. B **42**, 587 (1990).
[10]C. Leidlmair, Y. Wang, P. Bartl, H. Schöbel, S. Denifl, M. Probst, M. Alcamí, F. Martín, H. Zettergren, K. Hansen, O. Echt, and P. Scheier, Phys. Rev. Lett. **108**, 076101 (2012).
[11]H. Shin and Y. Kwon, J. Chem. Phys. **136**, 064514 (2012).
[12]C. Leidlmair, P. Bartl, H. Schöbel, S. Denifl, M. Probst, P. Scheier, and O. Echt, Astrophys. J. Lett. **738**, L4 (2011).
[13]Extensive hydrogenation of fullerene ions had been observed before,[14,15] but those studies did not reveal the formation of distinct adsorption layers.
[14]D. Schröder, D. K. Bohme, T. Weiske, and H. Schwarz, Int. J. Mass Spectrom. Ion Process. **116**, R13 (1992); S. Petrie, G. Javahery, J. Wang, and D. K. Bohme, J. Am. Chem. Soc. **114**, 6268 (1992).
[15]M. Farnik and J. Toennies, J. Chem. Phys. **122**, 014307 (2005).
[16]T. Oka, Proc. Natl. Acad. Sci. U.S.A. **103**, 12235 (2006).
[17]H. W. Kroto, J. R. Heath, S. C. O'Brien, R. F. Curl, and R. E. Smalley, Nature (London) **318**, 162 (1985); H. W. Kroto and M. Jura, Astron. Astrophys. **263**, 275 (1992).
[18]F. R. di Brozolo, T. E. Bunch, R. H. Fleming, and J. Macklin, Nature (London) **369**, 37 (1994).
[19]B. H. Foing and P. Ehrenfreund, Nature (London) **369**, 296 (1994); B. H. Foing and P. Ehrenfreund, Astron. Astrophys. **317**, L59 (1997).
[20]S. Petrie and D. K. Bohme, Astrophys. J. **540**, 869 (2000).
[21]G. H. Herbig, Astrophys. J. **542**, 334 (2000); A. Sassara, G. Zerza, M. Chergui, and S. Leach, Astrophys. J., Suppl. Ser. **135**, 263 (2001).
[22]X. K. Wang, X. W. Lin, M. Mesleh, M. F. Jarrold, V. P. Dravid, J. B. Ketterson, and R. P. H. Chang, J. Mater. Res. **10**, 1977 (1995).
[23]C. Jäger, F. Huisken, H. Mutschke, I. L. Jansa, and T. H. Henning, Astrophys. J. **696**, 706 (2009).
[24]J. Cami, J. Bernard-Salas, E. Peeters, and S. E. Malek, Science **329**, 1180 (2010); D. A. Garcia-Hernandez, A. Manchado, P. Garcia-Lario, L. Stanghellini, E. Villaver, R. A. Shaw, R. Szczerba, and J. V. Perea-Calderon, Astrophys. J. Lett. **724**, L39 (2010); J. Bernard-Salas, J. Cami, E. Peeters, A. P. Jones, E. R. Micelotta, and M. A. T. Groenewegen, Astrophys. J. **757**, 41 (2012).
[25]Y. Zhang and S. Kwok, Astrophys. J. **730**, 126 (2011).
[26]K. Sellgren, M. W. Werner, J. G. Ingalls, J. D. T. Smith, T. M. Carleton, and C. Joblin, Astrophys. J. Lett. **722**, L54 (2010).
[27]C. S. Jeffery, Astron. Astrophys. **299**, 135 (1995); D. A. Garcia-Hernandez, N. K. Rao, and D. L. Lambert, Astrophys. J. **729**, 126 (2011).
[28]K. R. G. Roberts, K. T. Smith, and P. J. Sarre, Mon. Not. R. Astron. Soc. **421**, 3277 (2012).
[29]T. P. Snow and B. J. McCall, Annu. Rev. Astron. Astrophys. **44**, 367 (2006).
[30]M. L. Heger, Lick Obs. Bull. **10**, 146 (1922).
[31]L. M. Hobbs, D. G. York, J. A. Thorburn, T. P. Snow, M. Bishof, S. D. Friedman, B. J. McCall, T. Oka, B. Rachford, P. Sonnentrucker, and D. E. Welty, Astrophys. J. **705**, 32 (2009).
[32]P. J. Sarre, J. Mol. Spectrosc. **238**, 1 (2006).
[33]J. P. Toennies and A. F. Vilesov, Angew. Chem., Int. Ed. **43**, 2622 (2004).
[34]L. An der Lan, P. Bartl, C. Leidlmair, H. Schöbel, R. Jochum, S. Denifl, T. D. Märk, A. M. Ellis, and P. Scheier, J. Chem. Phys. **135**, 044309 (2011).
[35]MATLAB R2011a, Mathworks, see http://www.mathworks.com.
[36]M. J. Frisch, G. W. Trucks, H. B. Schlegel *et al.*, GAUSSIAN 09, Revision A.02, Gaussian, Inc., Wallingford, CT, 2009; R. Ditchfield, W. J. Hehre, and J. A. Pople, J. Chem. Phys. **54**, 724 (1971).
[37]C. Adamo and V. Barone, J. Chem. Phys. **110**, 6158 (1999).
[38]J. P. Perdew, K. Burke, and M. Ernzerhof, Phys. Rev. Lett. **77**, 3865 (1996).
[39]N. Sai, K. Leung, and J. R. Chelikowsky, Phys. Rev. B **83**, 121309(R) (2011); e-print arXiv:1103.1938v1.
[40]C. Van Caillie and R. D. Amos, Chem. Phys. Lett. **328**, 446 (2000).
[41]S. Grimme, J. Comput. Chem. **27**, 1787 (2006); J.-D. Chai and M. Head-Gordon, Phys. Chem. Chem. Phys. **10**, 6615 (2008).
[42]S. E. Huber, S. Dalnodar, W. Kausch, S. Kimeswenger, and M. Probst, AIP Adv. **2**, 032180 (2012); M. P. Waller, H. Kruse, C. Muck-Lichtenfeld, and S. Grimme, Chem. Soc. Rev. **41**, 3119 (2012); Y. Zhao, X. J. Wu, J. L. Yang, and X. C. Zeng, Phys. Chem. Chem. Phys. **13**, 11766 (2011).
[43]See http://www.physics.nist.gov/PhysRefData/Elements/ for atomic element data.
[44]S. Jaksch, A. Mauracher, A. Bacher, S. Denifl, F. Ferreira da Silva, H. Schöbel, O. Echt, T. D. Märk, M. Probst, D. K. Bohme, and P. Scheier, J. Chem. Phys. **129**, 224306 (2008); P. Bartl, C. Leidlmair, S. Denifl, P. Scheier, and O. Echt, ChemPhysChem **14**, 227 (2012).
[45]T. T. Vehvilainen, M. G. Ganchenkova, L. E. Oikkonen, and R. M. Nieminen, Phys. Rev. B **84**, 085447 (2011).
[46]C. C. Henderson, C. M. Rohlfing, and P. A. Cahill, Chem. Phys. Lett. **213**, 383 (1993).
[47]T. Korona, A. Hesselmann, and H. Dodziuk, J. Chem. Theory Comput. **5**, 1585 (2009).
[48]P. A. Denis, J. Phys. Chem. C **112**, 2791 (2008).
[49]K. A. Williams, B. K. Pradhan, P. C. Eklund, M. K. Kostov, and M. W. Cole, Phys. Rev. Lett. **88**, 165502 (2002).
[50]C. M. Brown, T. Yildirim, D. A. Neumann, M. J. Heben, T. Gennett, A. C. Dillon, J. L. Alleman, and J. E. Fischer, Chem. Phys. Lett. **329**, 311 (2000).
[51]J. S. Arellano, L. M. Molina, A. Rubio, M. J. Lopez, and J. A. Alonso, J. Chem. Phys. **117**, 2281 (2002).
[52]I. Cabria, M. J. Lopez, and J. A. Alonso, Comput. Mater. Sci. **35**, 238 (2006).
[53]Y. Okamoto, J. Phys. Chem. A **105**, 7634 (2001); A. Ferre-Vilaplana, J. Chem. Phys. **122**, 104709 (2005); M. Rubes and O. Bludsky, ChemPhysChem **10**, 1868 (2009).
[54]P. A. Berseth, A. G. Harter, R. Zidan, A. Blomqvist, C. M. Araujo, R. H. Scheicher, R. Ahuja, and P. Jena, Nano Lett. **9**, 1501 (2009); T. X. Nguyen, J. S. Bae, Y. Wang, and S. K. Bhatia, Langmuir **25**, 4314 (2009).
[55]A. van Deursen and J. Reuss, Int. J. Mass Spectrom. Ion Phys. **11**, 483 (1973); Y. K. Bae, P. C. Cosby, and D. C. Lorents, Chem. Phys. Lett. **159**, 214 (1989); S. L. Anderson, T. Hirooka, P. W. Tiedemann, B. H. Mahan, and Y. T. Lee, J. Chem. Phys. **73**, 4779 (1980).
[56]A. A. Radzig and B. M. Smirnov, *Reference Data on Atoms, Molecules, and Ions* (Springer, Heidelberg, 1985).
[57]H. Tachikawa, Phys. Chem. Chem. Phys. **2**, 4702 (2000).
[58]Y. Ekinci, E. L. Knuth, and J. P. Toennies, J. Chem. Phys. **125**, 133409 (2006).
[59]W. K. Lewis, C. M. Lindsay, R. J. Bemish, and R. E. Miller, J. Am. Chem. Soc. **127**, 7235 (2005); A. M. Ellis and S. F. Yang, Phys. Rev. A **76**, 032714 (2007); O. Echt, T. D. Märk, and P. Scheier, in *Handbook of Nanophysics*, edited by K. Sattler (CRC, New York, 2010), Vol. 2; B. Shepperson, J. Liu, A. M. Ellis, and S. F. Yang, J. Chem. Phys. **135**, 041101 (2011).
[60]Penning ionization will dominate if the neutral dopant is located at the surface of the helium droplet, or if the electron energy is below the 24.59 eV threshold for formation of He^+.[61]
[61]A. A. Scheidemann, V. V. Kresin, and H. Hess, J. Chem. Phys. **107**, 2839 (1997); L. An der Lan, P. Bartl, C. Leidlmair, H. Schöbel, S. Denifl, T. D. Märk, A. M. Ellis, and P. Scheier, Phys. Rev. B **85**, 115414 (2012).
[62]E. Loginov, L. F. Gomez, N. Chiang, A. Halder, N. Guggemos, V. V. Kresin, and A. F. Vilesov, Phys. Rev. Lett. **106**, 233401 (2011).
[63]R. K. Yoo, B. Ruscic, and J. Berkowitz, J. Chem. Phys. **96**, 911 (1992).
[64]H. Schöbel, P. Bartl, C. Leidlmair, M. Daxner, S. Zöttl, S. Denifl, T. D. Märk, P. Scheier, D. Spångberg, A. Mauracher, and D. K. Bohme, Phys. Rev. Lett. **105**, 243402 (2010).
[65]O. Echt, D. Kreisle, E. Recknagel, J. J. Saenz, R. Casero, and J. M. Soler, Phys. Rev. A **38**, 3236 (1988).
[66]H. Steger, J. deVries, B. Kamke, W. Kamke, and T. Drewello, Chem. Phys. Lett. **194**, 452 (1992).
[67]A. J. Stace, J. Phys. Chem. A **106**, 7993 (2002).
[68]S. Denifl, F. Zappa, I. Mähr, F. Ferreira da Silva, A. Aleem, A. Mauracher, M. Probst, J. Urban, P. Mach, A. Bacher, O. Echt, T. D. Märk, and P. Scheier, Angew. Chem., Int. Ed. **48**, 8940 (2009); S. Denifl, F. Zappa, I. Mähr, A. Mauracher, M. Probst, J. Urban, P. Mach, A. Bacher, D. K. Bohme, O. Echt, T. D. Märk, and P. Scheier, J. Chem. Phys. **132**, 234307 (2010); H. Schöbel, C. Leidlmair, P. Bartl, A. Aleem, M. Hager, O. Echt, T. D. Märk, and P. Scheier, Phys. Chem. Chem. Phys. **13**, 1092 (2011).
[69]C. Leidlmair, P. Bartl, H. Schöbel, S. Denifl, T. D. Märk, S. Yang, A. M. Ellis, and P. Scheier, ChemPhysChem **13**, 469 (2011).
[70]J. H. Kim, D. S. Peterka, C. C. Wang, and D. M. Neumark, J. Chem. Phys. **124**, 214301 (2006); S. F. Yang, S. M. Brereton, M. D. Wheeler, and A. M. Ellis, J. Phys. Chem. A **110**, 1791 (2006); A. Boatwright, J. Jeffs, and A. J. Stace, *ibid.* **111**, 7481 (2007); H. Schöbel, P. Bartl, C. Leidlmair, S. Denifl, O. Echt, T. D. Märk, and P. Scheier, Eur. Phys. J. D **63**, 209 (2011).
[71]C. E. Klots, Z. Phys. D **21**, 335 (1991); R. Casero and J. M. Soler, J. Chem. Phys. **95**, 2927 (1991); K. Hansen and U. Näher, Phys. Rev. A **60**, 1240 (1999).

[72]C. E. Klots, J. Phys. Chem. **92**, 5864 (1988).
[73]C. Brechignac, P. Cahuzac, J. Leygnier, and J. Weiner, J. Chem. Phys. **90**, 1492 (1989); U. Näher and K. Hansen, *ibid.* **101**, 5367 (1994).
[74]J. Gspann, in *Proceedings of the 12th International Conference on the Physics of Electronic and Atomic Collisions*, edited by S. Datz (Gatlinburg, TN, 1981), p. 79.
[75]J. U. Andersen, E. Bonderup, and K. Hansen, J. Chem. Phys. **114**, 6518 (2001).
[76]S. Prasalovich, K. Hansen, M. Kjellberg, V. N. Popok, and E. E. B. Campbell, J. Chem. Phys. **123**, 084317 (2005).
[77]L. An der Lan, P. Bartl, C. Leidlmair, R. Jochum, S. Denifl, O. Echt, and P. Scheier, Chem.-Eur. J. **18**, 4411 (2012).
[78]The vibrational temperature of clusters in an evaporative ensemble is proportional to their binding energy, see Ref. 79. Helium droplets which have a dissociation energy of 0.62 meV cool to 0.37 K on a typical experimental time scale.[33] A temperature of 30 K will thus be expected if the evaporation energy is 50 meV.
[79]C. E. Klots, Nature (London) **327**, 222 (1987).
[80]U. Zimmermann, N. Malinowski, A. Burkhardt, and T. P. Martin, Carbon **33**, 995 (1995).
[81]S. Zöttl, A. Kaiser, P. Bartl, C. Leidlmair, A. Mauracher, M. Probst, S. Denifl, O. Echt, and P. Scheier, J. Phys. Chem. Lett. **3**, 2598 (2012).
[82]C. Kittel, *Introduction to Solid State Physics* (Wiley, New York, 2004).
[83]F. Calvo, Phys. Rev. B **85**, 060502(R) (2012).
[84]D. S. Greywall, Phys. Rev. B **47**, 309 (1993).
[85]J. de Vries, H. Steger, B. Kamke, C. Menzel, B. Weisser, W. Kamke, and I. V. Hertel, Chem. Phys. Lett. **188**, 159 (1992).
[86]See http://webbook.nist.gov/ for NIST Chemistry WebBook, 2012.